arXiv:0809.3142v2 [astro-ph] 9 Mar 2009

J. Fluid Mech. (2009), *vol.* 623, *pp.* 375–385. © 2009 Cambridge University Press
DOI: 10.1017/S000000000000000X Printed in the United Kingdom

Stratorotational instability in Taylor-Couette flow heated from above

M. GELLERT and G. RÜDIGER

Astrophysikalisches Institut Potsdam, An der Sternwarte 16, D-14467 Potsdam, Germany

(Received 2 September 2008 and in revised form 3 December 2008)

We investigate the instability and nonlinear saturation of temperature-stratified Taylor-Couette flows in a finite height cylindrical gap and calculate angular-momentum transport in the nonlinear regime. The model is based on an incompressible fluid in Boussinesq approximation with a positive axial temperature gradient applied. While both ingredients themselfs, the differential rotation as well as the stratification due to the temperature gradient, are stable, together the system becomes subject of the stratorotational instability and nonaxisymmetric flow pattern evolve. This flow configuration transports angular momentum outwards and will therefor be relevant for astrophysical applications. The belonging coefficient of β-viscosity is of the order of unity if the results are adapted to the size of an accretion disc. The strength of the stratification, the fluids Prandtl number and the boundary conditions applied in the simulations are well-suited too for a laboratory experiment using water and a small temperature gradient around five Kelvin. With such a set-up the stratorotational instability and its angular momentum transport could be measured in an experiment.

1. Introduction

In recent years instabilities in stratified media became of higher interest. Especially in view of astrophysical objects the inclusion of stratification is relevant. One simple model to study stratification effects is the classical Taylor-Couette (TC) system. Thorpe (1968) found a stabilizing effect of stratification only. In the context of stratorotational instability (SRI) stratification in TC flows is investigated numerically with fixed axial temperature gradient in a linear analysis studying the suppression of the onset of Taylor vortices by Boubnov et al. (1996). With fixed density gradient Molemaker, McWilliams & Yavneh (2001), Yavneh, McWilliams & Molemaker (2001) and Shalybkov & Rüdiger (2005) show the onset of a linear instability and the growth of nonaxisymmetric modes. Experiments using artifically enlarged buoyancy due to salt concentration (see Withjack & Chen 1974; Boubnov et al. 1995; LeBars & LeGal 2006) are in very good agreement with the linear results. Caton, Janiaud & Hopfinger (2000) use an artifical diffusivity in the continuity equation and show also results of linear stability analysis for the case of non-rotating outer cylinder. Umurhan (2006) analyses SRI analytically, especially the influence of vertically changing buoyancy frequency, in the quasi-hydrostatic semi-geostrophic limit. The author also shows that SRI survives only in the presence of no-slip radial boundary conditions. In the context of accretion disks, Dubrulle et al. (2005) figure out stability conditions and the influence of viscous dissipation and thermal diffusivity. In particular they find that the Prandtl number dependence of the critical parameters is unimportant. But fully nonlinear three-dimensional simulations do not exist. It is the aim of the first part of this paper to describe the characteristics of SRI in the nonlinear regime. The easiest way to do

nonlinear simulations is the application of an axial temperature gradient, where the top of the TC system has higher temperature than the bottom. The absence of a diffusivity in the continuity equation makes nonlinear simulations with explicit density gradient more demanding and favors a temperature gradient. Further on this is interesting also from an astrophysical view point: accretion disks are heated from the central object at their top and bottom. Thus the TC system heated from above could be seen as a simplified model for half of a disc. Of major interest for accretion or protostellar discs is the problem of angular momentum redistribution. Accretion only works if angular momentum is transported outwards effectively. Angular momentum transport of SRI is the second aspect of this work.

2. Model

The SRI is investigated in a model where stratification is due to a temperature gradient. At a first glance surprising this gradient is positive, i.e. the cylindrical gap is heated from above. This configuration, opposite to the negative gradient in Rayleigh-Bénard systems, is perfectly stable. The second ingredient in our model is differential rotation. The inner and outer cylinders rotate with different angular velocities. Both are chosen to be positive, i.e. exhibit the same direction of rotation. If the outer cylinder rotates sufficiently slow, the flow without temperature gradient evolves the well-known Taylor vortices for high enough Reynolds number. Beyond the Rayleigh line, when the outer cylinder rotates fast enough, the system is hydrodynamical stable. The combination of both stable parts can again drive the system unstable and generates a new instability, the SRI.

Stratification is measured by the Froude number

$$Fr = \Omega_{\rm in}/N, \tag{2.1}$$

the ratio between angular velocity of the inner cylinder and stratification given by the buoyancy frequency

$$N^2 = \alpha g \frac{\partial T}{\partial z} \tag{2.2}$$

Here α and g are the coefficient of volume expansion and gravity respectively, T is the temperature.

For the computations we fix the Froude number Fr, the cylinder height and the Prandtl number. In Rüdiger & Shalybkov (2008) it is shown that moderate stratifications are most effective. This means that for too strong stratification the instability is suppressed as well as for too low values. For the latter in the limit $Fr \to \infty$ the instability disappears in favor of the hydrodynamic stable configuration. Hence rotation and stratification of the same order, i.e. $Fr \approx 1$, appear to be a good choice to excite the instability. Rüdiger & Shalybkov (2008) find the optimum at $Fr = 1.4$, which is well-suited also for the nonlinear simulations presented here to get the smallest critical Reynolds numbers.

From an astrophysical point of view one of the most interesting questions arising is whether the SRI can transport angular momentum. If the normalized Reynolds stress $Q_{R\phi}/(R_{\rm in}\Omega_{\rm in})^2$, where $R_{\rm in}$ and $\Omega_{\rm in}$ are the inner radius and its angular velocity in cylindrical coordinates (R, ϕ, z) respectively, defined by the velocity fluctuations correlation

$$Q_{R\phi} = \langle U_R' U_\phi' \rangle, \tag{2.3}$$

turns out to be positive, angular momentum is transported outwards. This astrophysically important situation appears, as we show in § 5, always to be true in our simulations. Fluctuating quantities are defined as deviations from the azimuthally averaged mean

field, i.e. $\boldsymbol{U'} = \boldsymbol{U} - \langle \boldsymbol{U} \rangle$ with

$$\langle \boldsymbol{U} \rangle = \frac{1}{2\pi} \oint \boldsymbol{U} \, \mathrm{d}\phi. \tag{2.4}$$

Based on the idea, that angular momentum transport is mainly enhanced via an increase of viscosity, Shakura & Sunyaev (1973) introduce in a parameterized model for a disc a coefficient

$$\alpha_{\mathrm{SS}} = \frac{Q_{R\phi}}{H^2 \Omega_{\mathrm{in}}^2} \tag{2.5}$$

with the density scale height H of the disc. If the value of the α_{SS} is of the order of unity, the angular momentum transport is considered to be very effective and important. Taking the normalized Reynolds stress $\beta = Q_{R\phi}/(R_{\mathrm{in}}\Omega_{\mathrm{in}})^2$ for the SRI as an α-like coefficient, this leads to

$$\alpha_{\mathrm{SS}} = \beta \left(\frac{R_{\mathrm{in}}}{H} \right)^2 \approx \beta \cdot 10^3 \tag{2.6}$$

with the so-called β viscosity (see Lynden-Bell & Pringle 1974; Huré, Richard & Zahn 2000). Here is assumed that the SRI survives if the cylindrical container becomes larger in radial direction, which is not yet clear.

3. Equations and numerical treatment

We use a code based on the nonisothermal hydrodynamic Fourier spectral element code described by Fournier et al. (2005) and Gellert et al. (2007). With this approach we solve the 3D hydrodynamic equations in Boussinesq approximation

$$\partial_t \boldsymbol{U} + (\boldsymbol{U} \cdot \vec{\nabla}) \boldsymbol{U} = -\vec{\nabla} p + \vec{\nabla}^2 \boldsymbol{U} + Gr \, T \, \hat{\mathbf{e}}_z, \tag{3.1}$$

$$\partial_t T + (\boldsymbol{U} \cdot \vec{\nabla}) T = \frac{1}{Pr} \vec{\nabla}^2 T \tag{3.2}$$

$$\vec{\nabla} \cdot \boldsymbol{U} = 0 \tag{3.3}$$

for an incompressible medium in a cylindrical annulus with inner radius R_{in} and outer radius R_{out}. Free parameters are the Grashof number

$$Gr = \frac{Ra}{Pr} = \frac{\alpha g \Delta T D^3}{\nu^2} \tag{3.4}$$

and the Prandtl number $Pr = \nu/\chi$. Here ν is the viscosity of the fluid and χ its thermal conductivity. $D = R_{\mathrm{out}} - R_{\mathrm{in}}$ is the gap width. The Reynolds number appears not directly within the set of equations. It is defined, based on the inner cylinders angular velocity, as $Re = \Omega_{\mathrm{in}} R_{\mathrm{in}} D/\nu$ with the gap width D (used as unit of length) and the angular velocity of the inner cylinder Ω_{in}. Unit of velocity is ν/D and unit of time the viscous time D^2/ν.

The solution is expanded in M Fourier modes in the azimuthal direction. This gives rise to a collection of meridional problems, each of which is solved using a Legendre spectral element method (see e.g. Deville et al. 2002). Between $M = 8$ and $M = 32$ Fourier modes are used. The polynomial order is varied between $N = 8$ and $N = 16$ with three elements in radial direction. The number of elements in axial direction depends on the height of the cylinder, the spatial resolution is the same as for the radial direction. With a semi-implicit approach consisting of second-order backward differentiation formula and third order Adams-Bashforth for the nonlinear forcing terms time stepping is done with second-order accuracy.

At the inner and outer walls no heat-flux conditions are applied. In axial direction solid end caps with fixed temperatures T_0 and T_1 delimitate the cylindrical gap. The velocity

on both the inner and outer cylinders is fixed to $\Omega_{\rm in}$ and $\Omega_{\rm out}$ respectively. On the end caps stress-free conditions are applied to prevent Ekman circulation that would result from solid end caps rotating with the angular velocity of the inner or outer cylinder. This restriction is not essential for the occurrence of the instability, if the aspect ratio Γ is large enough. It simplifies the following analysis, because data along the full cylinder height can be included.

As initial flow profile we use the typical Couette profile

$$\Omega(R) = a + \frac{b}{R^2} \tag{3.5}$$

with

$$a = \frac{\mu - \eta^2}{1 - \eta^2}\Omega_{\rm in}, \qquad b = \frac{1 - \mu}{1 - \eta^2} R_{\rm in}^2 \Omega_{\rm in}, \tag{3.6}$$

the radius ratio $\eta = R_{\rm in}/R_{\rm out}$ and the ratio of angular velocities $\mu = \Omega_{\rm out}/\Omega_{\rm in}$. As initial temperature distribution the linear static advection profile is applied.

Without stratification the critical Reynolds numbers for an infinite cylinder with $\eta = 0.5$ is $Re_{\rm crit} = 68$ and $Re_{\rm crit} = 90$ for $\eta = 0.78$. With our simulations we find $Re_{\rm crit} = 69$ and $Re_{\rm crit} = 91$ respectively, which we decided to be in good agreement.

4. Onset of instability

The SRI occurs as instability leading to nonaxisymmetric flow patterns. After a linear growth phase, nonlinear interactions of the unstable modes occur resulting in a stable saturated state. The time the instability needs to evolve is around two viscous time scales D^2/ν or 120 system rotations, slightly depending on the Prandtl number. With $Pr = 1$ it needs slightly longer (150 rotations) and for $Pr \geqslant 7$ nearly 100 rotations. After saturation a stationary state is reached, where the flow pattern exhibits a drift compared to systems rotation. The growth rate of the instability is rather slow compared to other instabilities to produce (MHD-)turbulence like the magnetorotational instability (MRI, see Balbus & Hawley 1991) or Tayler instability (TI, see Tayler 1957; Rüdiger et al. 2007), where it is of the order of a few rotations. For both instabilities magnetic effects play an essential role. The SRI, even if slower, might be of comparable importance. As we will see in the following, it also leads to significant angular momentum transport. Further on stratification can suppress MRI or TI and thereby it becomes the most efficient instability mechanism in environments with weak or very strong magnetic fields. MRI and TI are suppressed by the strong magnetic field. Also in low-conducting environments like protostellar discs, where magnetic effects are unimportant, nonmagnetic instabilities could be of high relevance.

In our simulations we use two different gap sizes. The first one is a small gap with $\eta = 0.78$ also utilised in Shalybkov & Rüdiger (2005) and the second one is a wider gap with $\eta = 0.5$. Simulations are done with angular velocity ratios above the Rayleigh line. This means $\mu > 0.25$ for $\eta = 0.5$ and $\mu > 0.61$ for $\eta = 0.78$. Two special values, $\mu = 0.354$ for the wide gap and $\mu = 0.69$ for the small gap, are most interesting. These are the quasi-keplerian profiles, i.e. inner and outer cylinders would rotate like planets after the keplerian law $\sim R^{-3/2}$, in between the profile differs slightly from a keplerian. After the Rayleigh stability criterion $\partial_R (R^2\Omega)^2 > 0$ the configurations in our simulations are always hydrodynamically stable and the observed instability is due to the interplay between stratification and differential rotation.

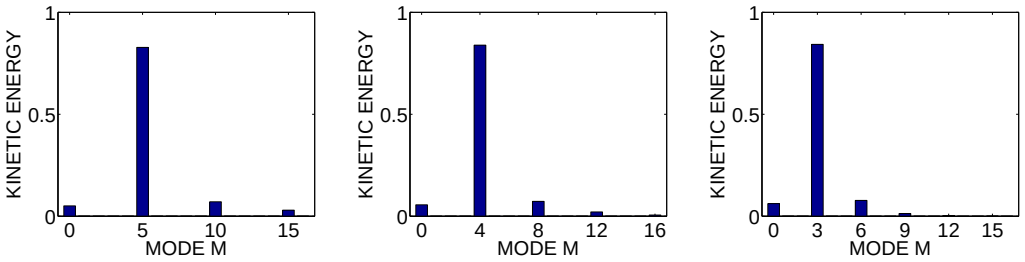

FIGURE 1. Histograms of Fourier modes for $Re = 500$, $Pr = 7$ in the small gap $\eta = 0.78$. The left plot is for $Fr = 0.7$, the middle for $Fr = 1$ and the right plot for $Fr = 1.4$. Shown is normalized total kinetic energy of the flow reduced by the driving due to the fixed cylinder rotation.

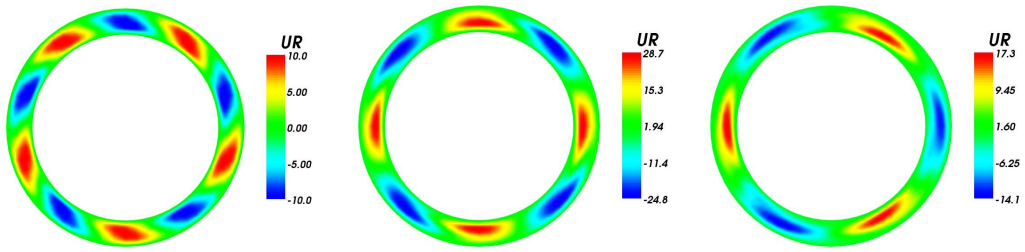

FIGURE 2. Contour plots of radial velocity component U_R in the midplane $z = \Gamma/2$ for $Re = 500, Pr = 7$ in the small gap $\eta = 0.78$. The plots are for $Fr = 0.7$, $Fr = 1$ and $Fr = 1.4$ from left to right respectively. The dominating Fourier mode is determined by the strength of the stratification.

4.1. *Wide gap*

The lowest critical Reynolds number for the onset of the instability is $Re = 285$ for $\eta = 0.5$, thus a rather weak stratification supports the SRI most effective. The most obvious difference between both gap sizes is the dominating unstable mode. For the wide gap it is always $m = 1$ in the observed parameter region $Re \leqslant 1000$, $1 \leqslant Pr \leqslant 10$ and $0.7 \leqslant Fr \leqslant 2$. All higher modes appear with gradual lower energy, where the step from mode m to $m+1$ is between 10 and 20% of the higher mode. So the spectrum decreases very fast.

4.2. *Small gap*

In the small gap case it is $m = 3$, $m = 4$ or $m = 5$ that become linear unstable and grows exponentially. The lowest critical Reynolds number here is $Re = 390$ for $Fr = 1.4$, again a weak stratification. When the unstable mode reaches a certain value, nonlinear effects appear and a wide range of modes become excited. After reaching the saturation level, the energy of the most unstable mode and of all harmonics stays constant, all other modes decay slowly on the thermal time scale. The most unstable mode depends mainly on the stratification. For decreasing $Fr = 1.4, 1.0, 0.7$ the mode with the largest growth rate changes from $m = 3$ to $m = 4$ to $m = 5$. And it is also this mode (and its harmonics) that dominates the saturated state (see figure 1 and figure 2). For $Fr = 1.6$ it is $m = 2$ that becomes the largest nonaxisymmetric mode and dominates the solution. For this rather low stratification one needs already a larger Reynolds number of $Re = 1000$ to trigger the instability. So this solution is not directly comparable to all three other cases with $Re = 500$. But the rule of decreasing m with increase of Fr is still valid.

The Prandtl number within the range $1 \leqslant Pr \leqslant 10$ has no obvious influence on the type of solution and the most unstable mode. Further on neither a variation of the Reynolds

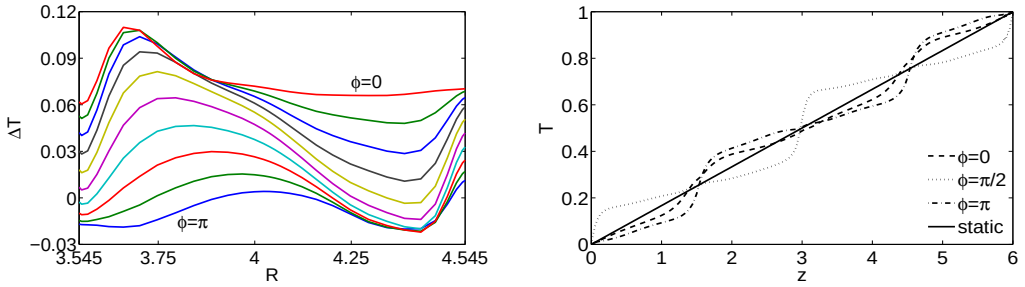

FIGURE 3. Radial and axial temperature profiles for $Re = 700, Pr = 7, Fr = 1.4$ in the small gap for several values of ϕ. Radial profiles are taken at half height and axial ones at the gap center. Deviations from the linear static profile are around 15%.

number (in the unstable regio) nor a variation of the steepness of the rotation profile μ has an obvious effect. This is different to the results in Shalybkov & Rüdiger (2005), where μ and Re have a clear effect on the stability of the several modes. Either the lines of marginal stability for the modes are so close to each other that a distinction in the nonlinear simulations is impossible, or the behavior changes remarkably when the stratification is increased further. The lowest Froude number reachable in the nonlinear simulations is $Fr = 0.7$ and the linear analysis uses a value of $Fr = 0.5$. Low Fr are more demanding because Ra increases quadratically with Fr and also Re needs to be larger and limits the accessible parameter space. Another aspect is in agreement with the linear analysis. Already for $\mu = 0.72$ we can not find an instability for $\eta = 0.78$ and $Re \leqslant 1000$, which is the maximum Reynolds number we can reach in our simulations. Thus, SRI feeds from an good balance between stratification and rotation with strong enough shear. The deviation from the linear static temperature profile is shown in figure 3. For a Reynolds number 1.5 times the critical one it differs significantly by around 15% from the linear profile. This effect becomes larger with increasing Re and vanishes near the onset of the stability.

5. Angular momentum transport

As shown in § 4, the variety of flow pattern is larger for the small gap container and might be a good choice for a laboratory experiment. Regarding angular momentum transport and its measurement a wider gap is favorable as we demonstrate in the following. With further aspects of an experimental realization is dealt in § 6.

5.1. *Wide gap*

By using equation (2.3) the Reynolds stress $Q_{R\phi}$ is calculated for a fixed set of parameters. A typical pattern in the $R-z-$plane is shown in figure 4 on the left. Angular momentum transport is always positive, i.e. directed outwards, with our configuration. The axial wave number varies between 4 and 12 for $\Gamma = 8$ depending mainly on the Froude number. Taking the value of $Q_{R\phi}$ in the gap center ($R = 1.5$) averaged along z gives the linear dependence on μ shown in figure 4 on the right. Thus the angular momentum transport depends linearly on the shear.

An increase of Fr leads to decreased angular momentum transport because maintenance of the instability needs a stronger driving flow for increasing stratification. If there exists an maximum of $Q_{R\phi}$ for given Fr with increasing Re like it is the case for angular momentum transport due to the Tayler instability of a toroidal magnetic field Gellert & Rüdiger (2008), is not easy to say. Within the accessible range of $Re \leqslant 1000$,

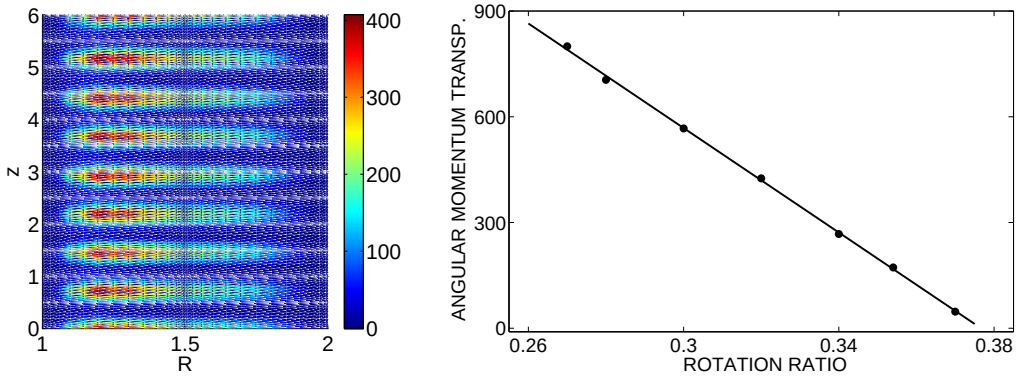

FIGURE 4. Pattern of Reynolds stress $Q_{R\phi} = \langle U_R' U_\phi' \rangle$ (left) for $\mu = 0.32$ and its linear dependence on shear (right). Angular momentum is transported outwards. Belonging parameters are $Re = 450$, $Pr = 1$, $Fr = 1$ and $\eta = 0.5$.

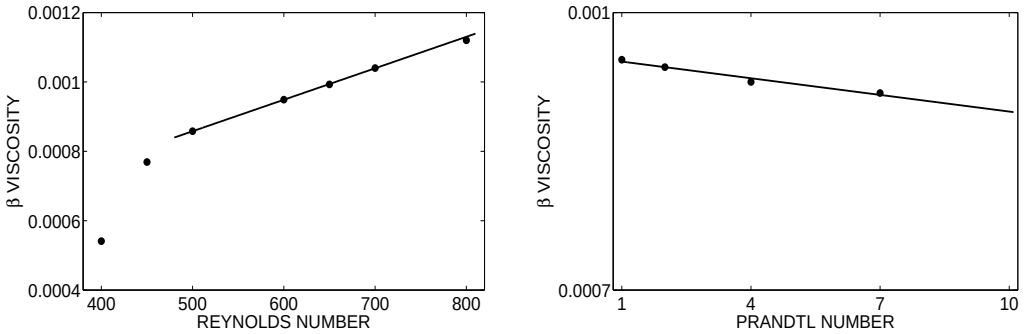

FIGURE 5. For $Fr = 1.4$, $\mu = 0.354$ and $\eta = 0.5$: on the left angular momentum transport in terms of the β viscosity at the gap center ($R = 1.5$) and averaged along z for $Pr = 1$. For Re not in direct vicinity of the stability boundary, β depends linear on Re. On the right side the weak dependence on the Prandtl number Pr is shown for $Re = 600$.

$Q_{R\phi}$ increases linearly with Re and without indication for saturation (see figure 5 left). A significant Prandtl number dependence can not be found (figure 5 right).

The nearly vanishing influence of Pr might be a sign for the fact, that it is not the convection-like temperature mixing that determines the SRI. This is only a secondary effect. The balance between centrifugal force and buoyancy is the crucial aspect. With $\chi \to 0$ and constant ν the instability appears without qualitative change. The effect is only a slight decrease of β. On the other hand if both ν and χ together are decreased (constant Pr and increasing Re), the β viscosity grows rapidly and linearly with Re, which means a scaling $Q_{R\phi} \propto \Omega^3$.

5.2. *Small gap*

Here the general behavior is the same as for the wide gap. The different nonaxisymmetric modes are not reflected in β. Compared with the small gap, the β viscosity is smaller by a factor of four but shows the same linear dependence on Re (see figure 6). The unimportant variation with the Prandtl number appears in the same way as for the wide gap for the observed Prandtl number range. This seems to be a very general behavior and is also reported for $Pr \geqslant 0.1$ by Dubrulle et al. (2005).

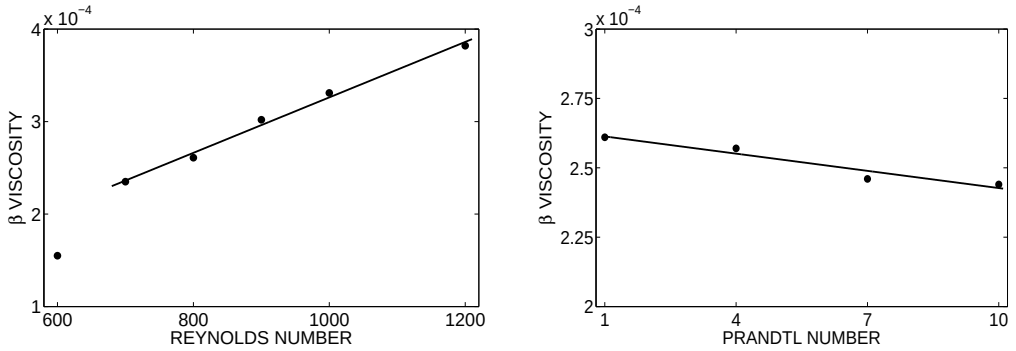

FIGURE 6. Same as in Fig. 5 but for the small gap with $\eta = 0.78$ and $Fr = 1.4$. It is for $Pr = 1$ on the left and $Re = 800$ on the right respectively.

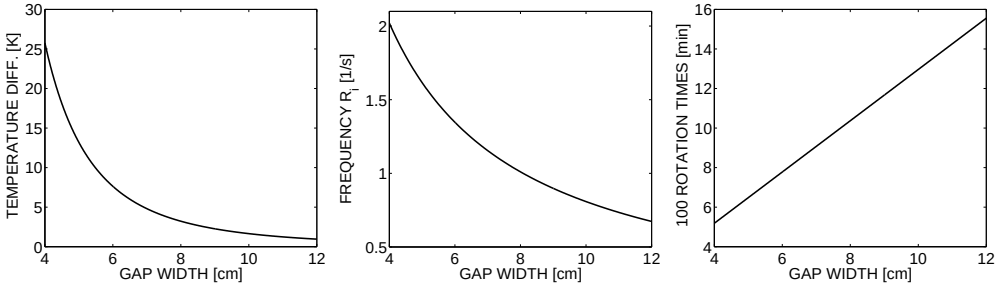

FIGURE 7. Needed temperature difference between top and bottom (left), rotation frequency of inner cylinder (middle) and time to reach the saturation level (right) for $\eta = 0.5$, $Re = 800$, $Fr = 1.4, \Gamma = 10$ and $Pr = 7.16$ (water).

6. Suggestion for a laboratory experiment

Experiments to study the SRI up to now use always a stratification accomplished by a salt solution. Test probes along the depth help to keep the stratification linear as good as possible. Even if the unstable system would evolve deviations from the linear profile (and it would in the nonlinear regime as shown in figure 3), this is suppressed and the profile is forced to stay unchanged. This disadvantage can be avoided by using a temperature gradient to realise a strong enough stratification. Here the boundary conditions are well defined and it is a rather easy task to keep them constant in time. There exist a lot of experience, for instance from Rayleigh-Bénard experiments and other convective systems to work with temperature gradients in the lab. That is why such a set-up is promising.

We show in the following of what size the TC system should be to reach appropriate stratifications and rotation speeds for water as working fluid. The Prandtl number of water is $Pr \approx 7$. For a possible set of parameters with $\eta = 0.5, Re = 500, \Gamma = 10$ and $Fr = 1.4$ one needs a Grashof number of $Gr = 1.3 \cdot 10^6$. This corresponds to a gap size of 6 cm for a temperature difference of 5 K or 9 cm for 2 K with water. Such dimensions for a TC system and the temperature difference are realizable in a laboratory. Figure 7 gives more details about dimensions, temperature differences and rotation frequency of possible experiments with the same parameters but $Re = 800$.

The crucial point seems to be the choice of the aspect ratio of the cylinders. On one hand one would like to extend the system to a high aspect ratio to limit perturbing effects from the end caps. On the other hand increasing height linearly increases the required temperature difference, because it is the derivative $\mathrm{d}T/\mathrm{d}z$ that controls the instability

and not the absolute value itself. Test simulations with solid end caps rotating with the angular velocity of the outer cylinder revealed that a smoothing of the pattern to axisymmetric structures near the top and bottom is inevitable, but it is the only effect if the aspect ratio is $\Gamma = 8$ or higher. Between 20% and 80% of the height the instability appeared in the same way as without solid end caps. Thus an aspect ratio of $\Gamma = 10$ might be an optimal choice for an experimental realisation.

Beneath the instability itself, also the transport of angular momentum should be possible to measure. A scenario to do so could be the following. The whole system is mounted on a rotation table rotating with the angular velocity of the inner cylinder. The outer cylinder has its own drive to realise the relative angular velocity difference. The inner cylinder is connected to the table only by using thin wires. If the instability occurs an additional torque acts on the inner cylinder and gives a measure for the β viscosity.

7. Discussion

We have shown fully nonlinear simulations of the SRI with temperature stratification in a cylindrical annulus. The stratification is stable, as well as the differentially rotating flow. Both together lead to unstable nonaxisymmetric modes. Depending on the gap width, these are the $m = 1$ or $m = 2/3/4/5$ modes in the investigated parameter range of rather weak stratification with Froude numbers around $Fr = 1$. Weak stratification results in the lowest critical Reynolds numbers for the onset of the SRI. On the other hand the instability is influenced by the Prandtl number of the flow only slightly. Especially the dominating mode m does not depend on Pr, only on Fr. The time the SRI needs to evolve and reach a saturated state is of the order of 120 rotations or two times the viscous time scale. Thus the growth rate of the instability is rather slow compared to magnetorotational instability and Tayler instability, where it is of the order of ten rotations. For both instabilities magnetic effects play the essential role. The SRI, even if slower, might be of comparable importance, when magnetic effects are rather unimportant or if stratification suppresses MRI or TI. Thus it might become the most efficient instability mechanism in environments with weak or very strong magnetic fields or in low-conducting environments like protostellar discs. We indeed find that SRI could be a mechanism able to transport angular momentum. The normalized angular momentum transport in terms of the β viscosity is of the order of 10^{-3}, in terms of the α_{SS} for a thin disk around unity. This comparison with a thin disk assumes that SRI still occurs in such a flat disk, which is not possible to answer with our simulations at the moment. Nevertheless is the size of β and its linear growth with Re a sign of significant influence of the SRI for angular momentum transport which might dominate over magnetic effects to produce turbulence in low-conducting environments. Beside astrophysical motivation angular momentum transport and turbulent transport coefficients are important also for technical applications. In tradition of the idea of Couette to measure viscosity of a fluid, the presented experimental configuration could be used to measure the transport of angular momentum or the increase of viscosity in the laboratory. With water it needs a TC system with $\Gamma \approx 10$ and a gap width of 6 cm to observe the SRI with a temperature difference between top and bottom of 5 K. For Reynolds numbers around $Re = 1000$ the time the instability needs to grow and to saturate is around 25 min or 120 rotations with 0.5 Hz. All these conditions seem to be appropriate for an experiment.

The authors would like to thank Rainer Hollerbach for stimulating discussions.

REFERENCES

Balbus, S. & Hawley, J. F. 1991 A powerful local shear instability in weakly magnetized disks. I - Linear analysis. II - Nonlinear evolution. *ApJ* **376**, 214–233.

Boubnov, B. M., Gledzer, E. B. & Hopfinger, E. J. 1995 Stratified circular Couette flow: instability and flow regime. *J. Fluid Mech.* **292**, 333–358.

Boubnov, B. M., Gledzer, E. B., Hopfinger, E. J. & Orlandi, P. 1996 Layer formation and transitions in stratified circular Couette flow. *Dyn. Atmos. Ocean* **23**, 139–153.

Caton, F., Janiaud, B. & Hopfinger, E. J. 2000 Stability and bifurcations in stratified Taylor-Couette flow. *J. Fluid mech.* **419**, 93–124.

Deville, M. O., Fischer, P. F. & Mund, E. H. 2002 *High Order Methods for Incompressible Fluid Flow*. Cambridge University Press.

Dubrulle, B., Marié, L., Normand, Ch., Richard, D., Hersant, F. & Zahn, J. P. 2005 A hydrodynamic shear instability in stratified disks. *Astron. Astrophys.* **429**, 1–13.

Fournier, A., Bunge, H.-P., Hollerbach, R. & Vilotte, J.-P. 2005 A Fourier-spectral element algorithm for thermal convection in rotating axisymmetric containers. *J.Comp. Phys.* **204**, 462–489.

Gellert, M., Rüdiger, G. & Fournier, A. 2007 Energy distribution in nonaxisymmetric magnetic Taylor-Couette flow. *Astron. Nachr.* **328**, 1162–1165.

Gellert, M. & Rüdiger, G. 2008 Toroidal field instability and eddy viscosity in Taylor-Couette flows. *Astron. Nachr.* **329**, 709–713.

Huré, J.-M., Richard, D. & Zahn, J.-P. 2001 Accretion discs models with the β-viscosity prescription derived from laboratory experiments. *Astron. Astrophys.* **367**, 1087–1094.

Le Bars, M. & Le Gal, P. 2006 Experimental Analysis of the Stratorotational Instability in a Cylindrical Couette Flow. *Phys. Rev. Lett.* **99**, id. 064502.

Lynden-Bell, D. & Pringle, J. E. 1974 The evolution of viscous discs and the origin of the nebular variables. *Mon. Not. R. Astron. Soc.* **168** 603–637.

Molemaker, M. J., McWilliams, J. C. & Yavneh, I. 2001 Instability and Equilibration of Centrifugally Stable Stratified Taylor-Couette Flow. *Phys. Rev. Lett.* **86**, 5270–5273.

Rüdiger, G., Hollerbach, R., Schultz, M., Elstner, D. 2007 Destabilisation of hydrodynamically stable rotation laws by azimuthal magnetic fields. *Mon. Not. R. Astron. Soc.* **377**, 1481–1487.

Rüdiger, G., & Shalybkov, D. 2008 Stratorotational instability in MHD Taylor-Couette flows. *Astron. Astrophys.*, accepted.

Shalybkov, D. & Rüdiger, G. 2005 Stability of density-stratified viscous Taylor-Couette flows. *Astron. Astrophys.* **438**, 411–417.

Shakura, N. I., & Sunyaev, R. A. 1973 Black holes in binary systems. Observational appearance. *Astron. Astrophys.* **24**, 337–355.

Tayler, R. J. 1957 Hydromagnetic Instabilities of an Ideally Conducting Fluid. *Proc. Phys. Soc. B* **70**, 31–48.

Thorpe, S. A. 1968 A method of producing a shear flow in a stratified fluid. *J. Fluid Mech.* **32**, 693–704.

Umurhan, O. M. 2006 On the stratorotational instability in the quasi-hydrostatic semi-geostrophic limit. *Mon. Not. R. Astron. Soc.* **365**, 85–100.

Withjack, E. M. & Chen, C. F. 1974 An experimental study of Couette instability of stratified fluids. *J. Fluid Mech.* **66**, 725–737.

Yavneh, I., McWilliams, J. C. & Molemaker, M. J. 2001 Non-axisymmetric instability of centrifugally stable stratified Taylor-Couette flow. *J. Fluid Mech.* **448**, 1–21.